Collective motion in Poly(ethylene oxide)/poly(methylmethacrylate) blends

Bela Farago*
Institute Laue Langevin, POB 156X 38042 Grenoble, France

Chunxia Chen and Janna K. Maranas
Department of Chemical Engineering, The Pennsylvania State University, University Park, Pennsylvania 16802, USA

Sudesh Kamath and Ralph H. Colby
Department of Materials Science and Engineering, The Pennsylvania State University, University Park, Pennsylvania 16802, USA

Anthony J. Pasquale and Timothy E. Long
Department of Chemistry, Virginia Polytechnic and State University, Blacksburg, Virginia USA
(Received 18 May 2005; published 29 September 2005)

We present neutron spin echo and structural measurements on a perdeutereted miscible polymer blend: poly(ethylene oxide)[PEO]/poly(methyl methacrylate)[PMMA], characterized by a large difference in component glass transition temperatures and minimal interactions. The measurements cover the q range 0.35 to 1.66 $Å^{-1}$ and the temperature range T_g−75 to T_g+89 K, where T_g is the blend glass transition. The spectra, obtained directly in the time domain, are very broad with stretching parameters $\beta \sim 0.30$. The relaxation times vary considerably over the spatial range considered however at none of the q values do we see two distinct relaxation times. At small spatial scales relaxations are still detectable at temperatures far below T_g. The temperature dependence of these relaxation times strongly resembles the β-relaxation process observed in pure PMMA.

DOI: 10.1103/PhysRevE.72.031809 PACS number(s): 61.41.+e, 64.70.Pf, 61.12.Ex

I. INTRODUCTION

Many materials do not crystallize and thus form an amorphous phase below their glass transition temperature T_g. Below this temperature, motion is greatly reduced and properties are dramatically altered. Two main classes of motion have been identified in amorphous systems. The primary or α-relaxation time becomes exceedingly long below the glass-transition temperature. In contrast, the β relaxation [also known as the Johari-Goldstein process or secondary relaxation] is active both above and below T_g. It follows an Arrhenius temperature dependence with no obvious change as T_g is crossed. Both processes coalesce in a temperature range 10–20 % above T_g with a single, merged relaxation observed at higher temperatures [1,2]. The dynamic processes of glass forming systems have been widely investigated using a variety of techniques including NMR [3,4], dielectric spectroscopy [5], and light [6], and neutron scattering [7,8].

Polymeric materials also form glasses, exhibiting the same general behavior described above. These motions are typically associated with segmental [α relaxation] or localized [β relaxation] processes. Whole chain motions, such as Rouse motion or reptation, also contribute to polymer dynamics, making the spectrum of dynamic processes in polymers very broad. Time-temperature superposition [tTS] is often used to extend the time scale of a polymer dynamics experiment by taking measurements at a series of temperatures. The premise of this principle is that lowering temperature has the same effect as extending to longer measurement times. tTS is often used with rheological data [9] but has also been applied to quasielastic neutron scattering data [10] using the shift factors obtained from rheology. The physical implication of shifting neutron data successfully with mechanical shift factors is that the processes probed by the two methods have the same temperature dependence, despite the fact that they probe very different time and spatial scales. The changes in motion that occur on blending of two polymers have been the focus of many investigations. Although one might expect a single dynamic response in a miscible mixture, studies show that two distinct α relaxations can be observed in miscible blends, usually when the T_g-s of the pure components are well separated [11–16]. At a fixed temperature, the usual observation is that the relaxation times will move closer to each other, i.e., the fast component is slowed and the slow component is accelerated. This is a consequence of the fact that the blend T_g will be intermediate between the T_g-s of the constituent components. The measurement temperature is closer to the blend T_g than the T_g of the fast component, and thus its motion is slowed in the blend. Similarly, the slow component is further from the blend T_g than its pure T_g, resulting in faster motion. α relaxations in miscible blends are typically broadened compared to the pure component response, which indicates that the range of dynamic time scales broadens on blending. One result of this is that time-temperature superposition [tTS] often fails in blends because the broadening increases as temperature is lowered.

In contrast to the α process, available data suggest that the β process is intramolecular and less affected by blending

*Email address: farago@ill.fr

[13]. Dielectric spectroscopy shows that neither the position nor the shape of the loss peak characteristic of the β relaxation of Poly Vinyl Methyl-Ether (PVME) is modified by blending with Polystyrene (PS) [13], whereas the α relaxation broadens considerably [17–21]. Also from quasielastic neutron scattering [22] it was found that the methyl group rotation of poly(vinyl methyl ether) is hardly sensitive to blending with polystyrene. All of this indicates the β relaxation is less affected by blending than the α relaxation. Most theories of dynamics in miscible blends are based on the idea that within a certain [small] volume surrounding a given segment, there is a local composition that is different than the bulk composition. This results in distinct dynamic behavior for each component, and a broadened α process [12,21,23–26].

II. LITERATURE ON DYNAMICS OF PEO/PMMA BLENDS

We investigate mixtures of poly(ethylene oxide) [PEO, $T_g \sim 221$ K] and poly(methyl methacrylate) [PMMA, $T_g \sim 402$ K]. This blend is characterized by large T_g contrast [$\Delta T_g \sim 181$ K] and minimal interactions [27]–the Flory χ parameter is nearly zero. A variety of techniques have been employed to study the dynamics of this blend, including dielectric spectroscopy [28], NMR [29], and mechanical spectroscopy [9]. The two components retain their individual characters in the blend, as suggested by deuterium-NMR measurements [29] and the failure of tTS in oscillatory shear measurements [9]. Dielectric spectroscopy on blends with PEO contents up to 25 wt % shows that the merged $\alpha\beta$ relaxation process of PMMA becomes faster with the addition of PEO, the low-T_g component [30]. This study also suggests that PEO motion is cooperative with the main chain of PMMA. In contrast, NMR on d_4PEO/PMMA blends with PEO contents of 3–30 % has observed PEO motion that is up to 12 orders of magnitude faster than PMMA motion at the blend T_g, and depends only weakly on composition [29], suggesting the motion of PEO is not coupled to that of PMMA. These authors ascribe their observations to the lack of side groups in PEO allowing it to move freely on the segmental level, despite being surrounded by nearly immobile PMMA chains. Another explanation is provided by Ref. [12]. Concentration fluctuations [which should be important in this blend due to its small χ parameter] temporarily create regions rich in PEO, which allow a fraction of the PEO to relax unhindered by PMMA. Another fraction of the PEO would be expected to relax more slowly, consistent with the mean blend composition, leading to a bimodal distribution of relaxation times, as is sometimes observed for the low-T_g component in miscible blends [12].

Using oscillatory shear rheometry [9,24], Colby studied the temperature dependence of the terminal relaxation times for both components in blends with 20 and 30 wt % PEO. At any given temperature, the two relaxation times are shifted toward each other in the blend, but if considered at constant $T-T_g$, PMMA [the slow component] is less mobile in the blend. The PEO relaxes slightly faster, although the difference is small and could be interpreted as no change in mobility when blended. These results were obtained in the range T_g+40 to T_g+100 K. The data cannot be superposed and this is attributed to the separate friction factors for each component. Zawada *et al.* [24] used simultaneous measurements of infrared dichroism and birefringence to monitor the dynamic response of this blend with PEO contents ranging from 40 to 80%. In this composition range, PEO dynamics are slowed considerably at constant $T-T_g$, while the change in PMMA dynamics is smaller and non-monotonic in composition. These data, taken with the oscillatory shear data, present a complicated composition dependence of terminal dynamics in this blend.

The dynamic behavior of both pure components has also been investigated. Results from broadband dielectric spectroscopy are able to discern both the α and β relaxations of pure PMMA around T_g [28]. Near T_g the α-relaxation time changes very rapidly with temperature and the β-relaxation time follows an Arrhenius temperature dependence with an activation energy of $E_a=79$ kJ/mol. The β relaxation of pure PMMA has been attributed to hindered rotation of the carboxyl side group around the bond that links it to the main chain [28]. Pure PEO has been investigated using quasielastic neutron scattering [31–33]. However these studies were concentrating on PEO/alkali complexes and all measurements were done above the melting temperature of PEO, which occurs near T_g+120 K.

Quasielastic neutron scattering provides temporal and spatial information by following both the energy [time] and momentum [spatial] changes of the neutrons interacting with the sample. Potentially it offers the possibility to follow the motions from local to mesoscopic scales as well as to identify the moving part. Two types of experiments are possible: incoherent, which measures self-motion, and coherent, which measures the collective relaxation [relative motion]. In the first case some molecules or parts of the molecules are labeled with hydrogen while the others are synthesized with deuterium. The high incoherent scattering of the hydrogen usually dominates at large wave vectors, thus allowing the observation of the self motion of the labeled part. When some polymer chains are hydrogen labeled in a matrix of deuterated chains, in addition there is a strong coherent scattering at small wave vectors arising from the contrast between the coherent scattering length densities of the protonated and deuterated chains. Finally when all the chains are deuterated one observes the collective relaxation at large wave vectors. The self-motion of PMMA in the PEO/PMMA blend has been studied very recently [34]. This work shows that the main effect of blending on the dynamics of PMMA is a shift of T_g. When this difference is taken into account the relaxation curves collapse on a single master curve. Incoherent scattering is not well suited for neutron spin-echo (NSE) partly because of the weak intensity, but more importantly the $-1/3$ polarization of the hydrogen incoherent scattering is very unfavorable for the signal-to-noise ratio. The current work presents results on the collective relaxation (coherent scattering) obtained from NSE measurements. As we will show in the following the contribution from the two polymers to the scattered intensity varies as a function of q thus from the wave-vector dependence of the relaxation we expected to observe whether the two components show distinct relaxation times or not.

TABLE I. Properties of samples.

Polymers	M_w	Polydispersity	Deuterium level (%)	T_g(K)
dPEO	550 000	<1.1	99.89	221
dPMMA	375 000	<1.2	99.54	402

The NSE technique has been applied to several single component polymers at large q: polybutadiene [2,10], polyisobutylene [10,35–37], and polypropylene [38]. Relaxation times for polybutadiene at the first (interchain) and second (intrachain) peaks in the static structure factor show temperature dependences that can be associated with the α and β processes, respectively. This is further evidenced by the success of tTS (using shift factors from mechanical data) at the interchain peak, and failure at the intramolecular peak. These results support the idea that at the interchain peak, NSE probes essentially the high frequency tail of the α process, while some other, more local processes start to contribute at higher q, such as at the intrachain peak. Only measuring the collective relaxation (coherent scattering) permitted to link the fundamental change in dynamics to the type of correlation (inter-, intra-chain). One study [15] has investigated polymer blend dynamics in the Polyisoprene/Poly(vinylethylene) (PI/PVE) system far above T_g. The NSE measurements focused on chain motion at small wave vectors, and were converted to incoherent relaxation times using the Rouse model for comparison to backscattering measurements. The results showed that at temperatures far above the blend T_g, the component relaxation times coincide at length scales greater than 31 Å, and differ at length scales of 14 Å and less [15].

In the current study, we focus on the large q range, similar to that of the inter- and intra-chain peaks in $S(q)$, as in the pure component studies discussed above. The PEO/PMMA blends we measured had 0, 10, 20, and 30 wt % PEO and were investigated from 273–414 K [below and above the blend T_g] and in the q range 0.35 to 1.66 Å^{-1}. The q range covers the structure factor peaks of both PEO and PMMA, and is in the region where distinct component mobilities are expected [15].

III. EXPERIMENT

A. Materials and sample preparation

Perdeuterated PEO/PMMA blends and perdeuterated pure PMMA were used for the experiments. Both components were prepared by anionic polymerization and thus have narrow molecular weight distributions and yield 80% syndiotactic PMMA. The dPEO was obtained from Polymer Laboratories (Amherst Fields Research Park, 160 Old Farm Road, Amherst, MA, 01002). PMMA was prepared as follows. The deuterated MMA (Aldrich) was distilled under reduced pressure from both calcium hydride and triethylaluminum to ensure complete removal of protic impurities. The purified monomer was added to a reactor containing tetrahydrofuran (THF) at −78 °C and diphenylhexyllithium as an initiator. The monomer was added drop wise to minimize exotherms which would lead to premature termination. The polymerization was allowed to proceed for 20 min at −78 °C after complete addition of the MMA monomer. The polymerization was terminated with the addition of acidic methanol. The THF solution (approximately 10% polymer by weight) was precipitated in excess petroleum ether and upon filtration, the sample was dried for 18 h at 60 °C under reduced pressure. The white fibrous product was obtained in greater than 95% isolated yield. The weight-average molecular weights, deuterium level, polydispersity indices, and glass transition temperatures for both components are given in Table I. Deuterium levels were assessed with proton NMR. Differential scanning calorimetry (DSC) with heating and cooling rates of 10 K/min was used to measure the glass transition temperatures. The T_g for the 10, 20, and 30 wt % blend are 365, 348, and 326 K. T_g of pure PMMA is 402 K and T_g =221 K for PEO. Polydispersity was assessed using size exclusion chromatography. The blend samples were prepared using the following procedure. The required amounts of PEO and PMMA were calculated and each component was dissolved separately in acetone at 313 K with constant stirring using a magnetic stirrer for 8 h. Once both polymers had dissolved completely in the solvent, the solutions were mixed and the mixture was stirred for an hour. This solution was then transferred to a round-bottomed flask and dried in a rotary evaporator at 313 K. The resulting mixture was further dried in a vacuum oven at 423 K for three days to remove any residual solvent. The sample was rapidly transferred to a hot press maintained at 410 K and hot pressed for 4 h. Once the sample had been pressed, the entire hot press assembly was quenched in liquid nitrogen to prevent crystallization. The resulting samples were transparent with single, albeit broad glass transitions in (DSC), indicating miscibility.

PEO is a semicrystalline polymer. Zawada *et al.* [24] reported that $T_m \approx 338$ K decreases to ≈ 330 K in a 50–50 % blend. However form our experience in the blends where $T_g \geqslant T_m$ there is no problem of crystallization. With DSC by keeping the sample at 25 °C for a long time we could not see visible melting endotherm. So we can safely say that considerably less than 1% of the PEO is crystalline but of course there is no way to prove there is strictly zero crystallinity. We can also mention that the neutron diffraction repeated several months later did not show any change in the structure neither.

B. Methods

NSE measures the velocity change of incident and scattered neutrons using the Larmor precession of the neutron spin in an external magnetic field. Details of the method are given elsewhere [39]. The directly measured quantity by the

NSE technique is the normalized dynamic structure factor in the time domain

$$\tilde{S}(q,t) = \frac{I(q,t)}{I(q,0)} = \frac{\sum_{ij} \langle b_i b_j \exp[i\vec{q} \cdot \vec{r}_{ij}(t)] \rangle}{\sum_{ij} \langle b_i b_j \exp[i\vec{q} \cdot \vec{r}_{ij}(0)] \rangle}, \quad (1)$$

where $\vec{r}_{ij}(t) = \vec{r}_j(t_0+t) - \vec{r}_i(t_0)$ and i and j indicate different scattering centers. The strength of the neutron/nuclei interaction is characterized by the scattering length b_i. The averaging $\langle\ \rangle$ is taken over the initial time t_0 (thermal average of the initial positions). The momentum transfer $q = \frac{4\pi}{\lambda}\sin(\frac{\theta}{2})$ (θ: scattering angle) is related to the spatial scale probed in the experiment: $r = 2\pi/q$.

The NSE experiments were performed at the NSE spectrometer IN11C [40] at the Institute Laue-Langevin (ILL) in Grenoble, France. The wavelength of the incoming neutrons was $\lambda = 5.76$ Å with $\Delta\lambda/\lambda = 15\%$ full width half maximum (FWHM). The instrumental resolution was measured on amorphous quartz with a similar shape and size as the sample as well as on the samples themselves by cooling them down to 10 K where all relaxations can be safely supposed to be frozen out. Data were taken with the double echo configuration [41,42] between Fourier times of 0.008 and 1.48 ns with roughly equidistant steps on a logarithmic scale. The 10–30 % PEO/PMMA blends were studied at six temperatures: $T = 273$, 313, 352, 371, 393, and 413 K while the pure PMMA sample was measured only at 293 and 413 K. IN11C is equipped with a multidetector bank covering a 30° scattering angle in one position. Combining three detector positions allowed gathering of data over a q range of 0.35 to 1.66 Å^{-1}. At each position the 40 detectors were binned into seven groups each covering about a 4.3 deg scattering angle.

The static structure factors $S(q)$ for the blends and pure PMMA were measured on the D20 diffractometer at the ILL at room temperature. Since there are few protons present in the samples, the scattering intensity for both structural and dynamic experiments is dominated by coherent scattering. In the static structure factor, this reveals preferred packing distances, and in NSE spectra collective motion between different scattering centers is observed. The dynamic structure factor in Eq. (1) can be split into partial structure factors

$$I(q,t) = \sum_{\substack{i\in\mathrm{PMMA} \\ j\in\mathrm{PMMA}}} \langle b_i b_j \exp[i\vec{q} \cdot \vec{r}_{ij}(t)] \rangle + 2 \sum_{\substack{i\in\mathrm{PEO} \\ j\in\mathrm{PMMA}}} \langle b_i b_j \exp[i\vec{q} \cdot \vec{r}_{ij}(t)] \rangle + \sum_{\substack{i\in\mathrm{PEO} \\ j\in\mathrm{PEO}}} \langle b_i b_j \exp[i\vec{q} \cdot \vec{r}_{ij}(t)] \rangle,$$

$$I(q,t) = I_{\mathrm{PMMA-PMMA}}(q,t) + 2I_{\mathrm{PEO-PMMA}}(q,t) + I_{\mathrm{PEO-PEO}}(q,t), \quad (2)$$

where again $\vec{r}_{ij}(t) = \vec{r}_j(t_0+t) - \vec{r}_i(t_0)$. If one component (e.g., the PMMA) is immobile then the time average over t_0 in the first two contributions will yield $S(q)_{\mathrm{PMMA-PMMA}}$ and $S(q)_{\mathrm{PEO-PMMA}}$, and thus should show up as an elastic contribution, while the third term should reflect the mobility of PEO. This statement might look nontrivial for the cross term. Indeed, for example, if $i \in$ PMMA then $\vec{r}_i(t_0)$ will be independent of t_0. However when the position of the mobile atom $\vec{r}_j(t_0+t)$ is averaged over t_0 it will include all possible configurations in space and thus there is no t dependence left. In other words, taking the time average is the same as taking the ensemble average, which must yield $S(q)$. On the other hand we will observe a mixing of the relaxation times (from the cross term) if *both* components are mobile in our time window.

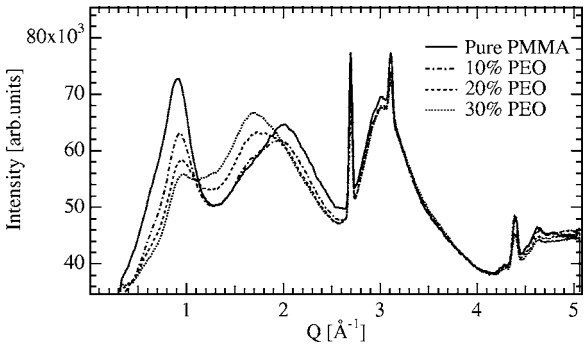

FIG. 1. Static structure factor of perdeuterated pure PMMA and 10, 20, and 30 % dPEO/ dPMMA blends.

Our approach is very different from the one employed in Ref. [15]. There hydrogen labeling was used to highlight one or the other blend components for backscattering at high q and the self-relaxation was measured. At low q NSE measured the single chain (coherent) dynamics of the labeled component and the results were converted to the self-relaxation times, to compare and extend the backscattering data to lower q values. In our work we concentrate on the coherent collective dynamics at high q and we expect to identify the origin of the movement by examining the change in the static structure factor upon blending at the same q values.

IV. RESULTS

A. Structure

Shown in Fig. 1 is the coherent static structure factor $S(q)$ for perdeuterated pure PMMA and perdeuterated 10, 20, and 30 % dPEO/dPMMA blends at room temperature. As the quantity of the samples in the beam was not identical, we rescaled the scattered intensities to overlap in the 2.8–4.2 Å^{-1} range. These length scales ($r < 2.5$ Å) correspond to distances involving a few bond lengths and angles, neither of which are expected to, and visibly do not, vary significantly with blend composition. The sharp Bragg peaks at 2.7, 3.1, and 4.39 Å^{-1} are due to the aluminum sample holder. Pure dPMMA is characterized by a first peak at $q = 0.9$ Å^{-1}, and two broad peaks at $q = 2.0$ and 3.0 Å^{-1}. The locations of these peaks are consistent with the coherent static structure factor observed by Moreno *et al.* [43] for

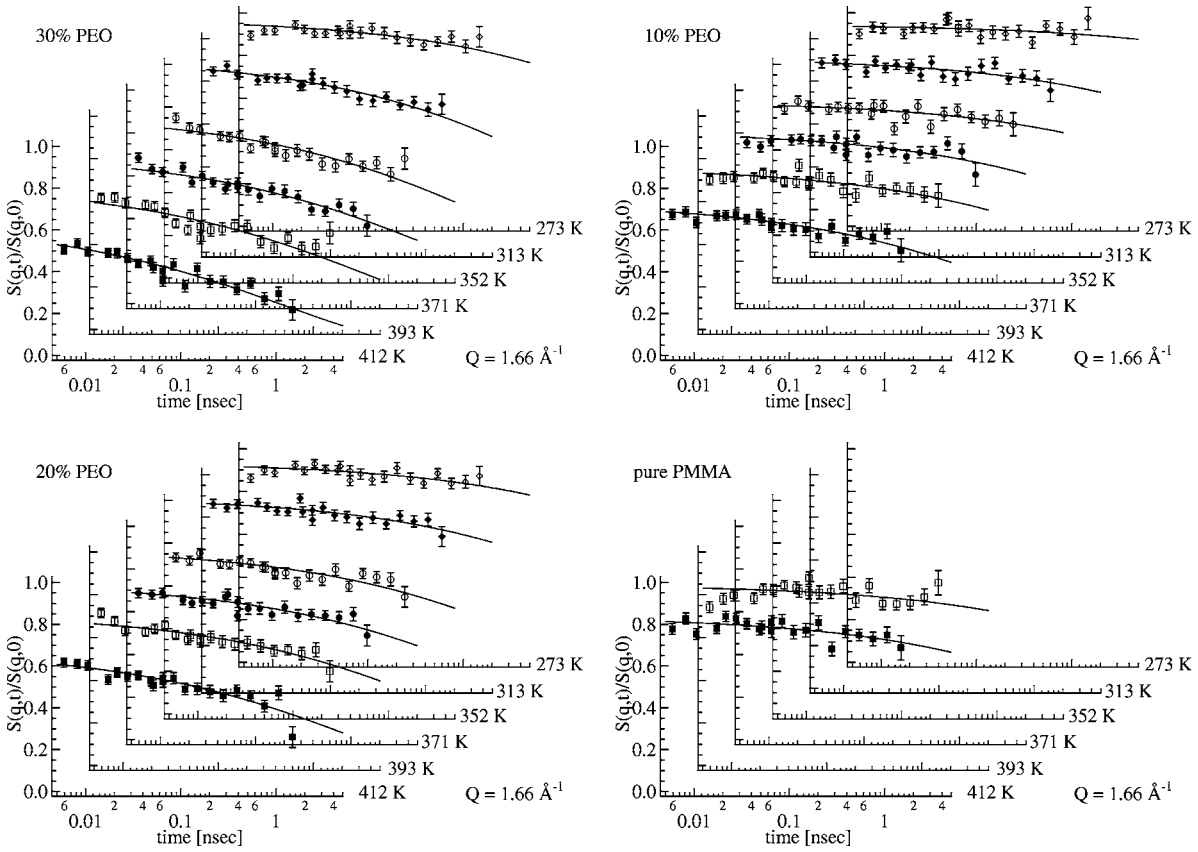

FIG. 2. Dynamic structure factor of perdeuterated dPEO/dPMMA blends 30% (a), 20% (b), 10% (c), and pure dPMMA (d) at Q $=1.66$ Å^{-1}. Lines are the KWW fits with $\beta=0.3$.

PMMA with all hydrogens except those of the $COOCH_3$ group substituted with deuterium. Thus most likely origin of the first peak ($q=0.9$ Å^{-1}) is intermolecular PMMA correlations. The second broad peak at $q=2.0$ Å^{-1} is consistent with intramolecular packing of the PMMA backbone segment and the side group with which it is bonded. The fact that it is broader than the first peak indicates a broader distribution of atomic pair distances, and also that the side group samples a number of different configurations with respect to the chain backbone. Rotation of the $COOCH_3$ side group around the C-C bond linking the side group to the main chain has been identified as the origin of the β relaxation in pure PMMA [44], and thus expected to stay active even below T_g.

We now consider the effect on packing when PEO is added to pure PMMA. The intermolecular chain packing peak in pure PEO occurs at $q=1.4$ Å^{-1}, as assessed by neutron diffraction [45], and molecular dynamics simulation [46]. The peak at 3.0 Å^{-1} does not change its shape or location with PEO content, as is consistent with a specific intramolecular atom pair separated by at most two bonds. The peak at 0.9 Å^{-1} gradually decreases in height with PEO content. In the 1.2–1.8 Å^{-1} region we observe an increase of intensity, though only for more than 10% PEO content. This region roughly corresponds to the pure PEO chain packing peak of 1.4 Å^{-1}. On the other hand, in the 2.0–2.5 Å^{-1} region there is a sudden change when going from 0 to 10 % PEO content and no more change after. We explain these observations the following way. If we start adding PEO it will be first distributed homogeneously in the PMMA matrix, thus introducing more disorder for the PMMA-PMMA backbone correlations ($q=0.9$ Å^{-1}) but the 10% quantity is not yet sufficient to show significant PEO-PEO correlations (1.2–1.8 Å^{-1}). The sudden change in the 2.0–2.5 Å^{-1} region might indicate some preferential sites of the PEO chains relative to the PMMA, but these sites become fully occupied by 10% PEO. Addition of more PEO changes little the intensity in this region while the PMMA interchain correlation diminishes and the PEO-PEO correlation at 1.2–1.8 Å^{-1} builds up. If the PEO in the blend maintains the mobility of pure PEO, based on the observations above we expect this to be the best visible in the 1.2-1.8 Å^{-1} q range.

B. Dynamics

Examples of NSE spectra of different compositions and temperatures at a selected high q are presented in Fig. 2. Figure 3 shows a low q value where the pure PMMA and the 10% blend are practically elastic and the 20 and 30 % blends show some decay on the borderline of what can be detected in our time window. The curves in the figure are Kohlrausch-Williams-Watts (KWW) or stretched exponential fits

$$\frac{S(q,t)}{S(q,0)} = A(q)\exp\left[-\left(\frac{t}{\tau_{\mathrm{KWW}}(q)}\right)^{\beta}\right], \tag{3}$$

where $\tau_{\mathrm{KWW}}(q)$ is the characteristic relaxation time, and β is the stretching exponent, representing the deviation of the ob-

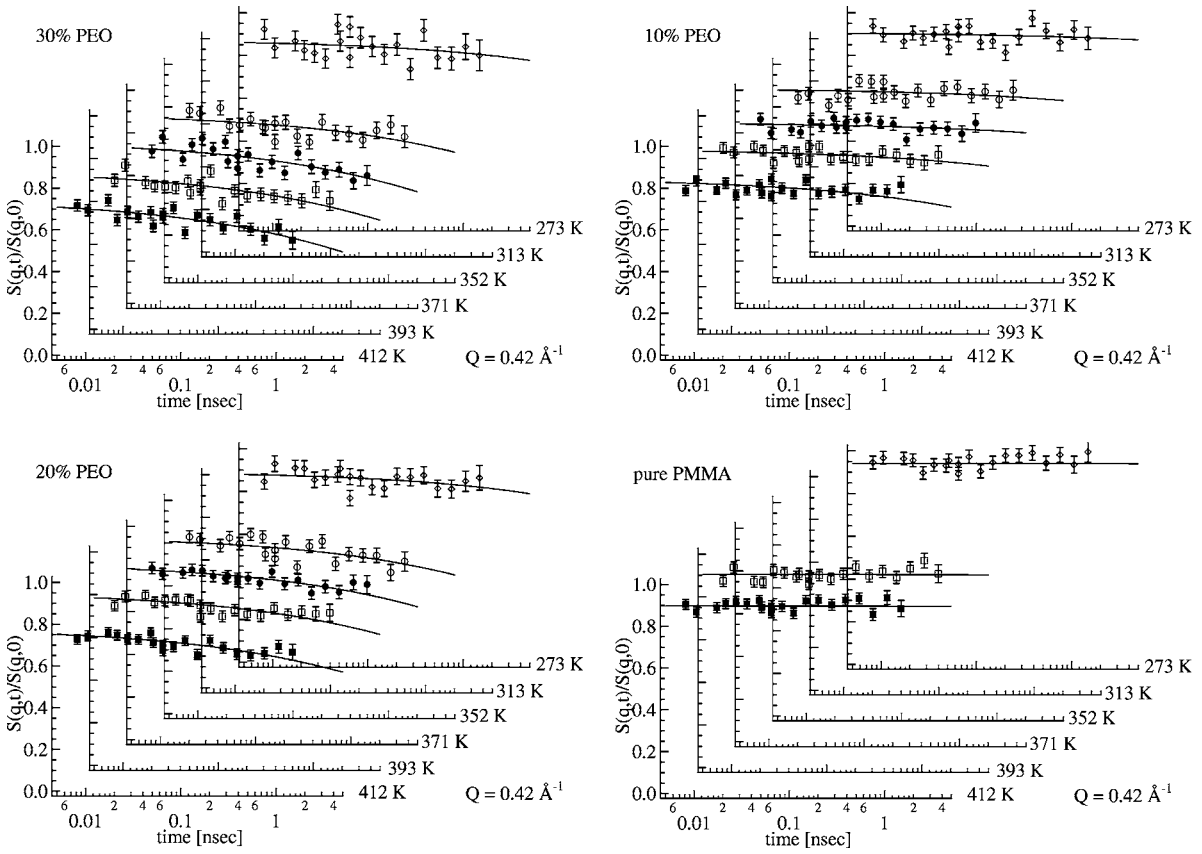

FIG. 3. Dynamic structure factor of perdeuterated dPEO/dPMMA blends 30% (a), 20% (b), 10% (c), and pure dPMMA (d) at Q $=0.42$ Å^{-1}. Lines are the KWW fits with $\beta=0.3$.

served relaxation process from a single exponential relaxation ($\beta=1$). If the prefactor $A(q)<1$, it means that there are dynamic processes occurring at time scales shorter than our experimental window but still in the bandpass of the instrument. In the case of IN11C for our configuration this corresponds to the energy band of 0.2–2.5 meV. This energy range includes contributions from local vibrations, overdamped phonons, and in some cases part of the so-called boson peak.

The relaxation processes we observe are very stretched at all momentum transfers. For pure glasses where tTS applies, usually one can superimpose several temperatures and from such spectra, covering four to five decades in rescaled time, one can determine the β exponent with good confidence. For our PEO/PMMA blend, based on rheology, tTs cannot be used because mechanical data cannot be superposed. Our methodology in fitting the data to Eq. (3) is to first fit the data with the most pronounced decay (high temperature, high q spectra) with all three parameters floating. Such obtained β values scatter around 0.2–0.4. What we can safely state is that if Eq. (3) holds then $0.15 \leqslant \beta \leqslant 0.4$. As no clear trend emerged for an eventual q or T dependence of β, we took fixed values of β between 0.15 and 0.4 by steps of 0.05 and fitted all spectra with $A(q)$ and $\tau_{\mathrm{KWW}}(q)$ as fit parameters in order to see how the global goodness of fit (χ^2) evolves. The reason to work with a fixed β is that β and $\tau_{\mathrm{KWW}}(q)$ are strongly correlated in the fitting and a variable β could lead to hidden artifacts. This evidently means that a fixed β can as well introduce artifacts if in reality it is *not* constant. We found that χ^2 decreases with decreasing β, however the decrease is not very significant. For the 30% sample, where the decays are the most significant, χ^2 decreases from 1.6 at $\beta=0.4$ to 1.3 at $\beta=0.15$. To make the best choice we have to further scrutinize the q and temperature dependence of the $A(q)$ parameter. As mentioned above $A(q)$ comes from higher energy processes thus not only does it have to be less than 1.0 but also with increasing temperature it can only decrease or stay constant. These conditions are not always met by the fit results for $\beta<0.2$. In the following we will present the fit parameters obtained with a fixed median value of $\beta=0.3$, but where it is important we will mention the dependence on the choice of β. Many of our spectra show only a small decay. To further reduce data scatter, we tried to draw a smooth curve (third-order Chebyshev polynomial) on the q dependence of the prefactor, which is not expected to change rapidly, and refitted the decay times with these fixed prefactors. Scatter was somewhat reduced, but within the calculated error bars. In the following these decay times will be presented and discussed. To place an upper limit on the relaxation times that can be extracted with reasonable confidence from the data, we require that the spectra has decayed at least 7% from its initial value. This is about the limit where even with very good statistics instrumental systematic errors start to play a role. Because of the small β exponent (0.3), this sets an upper limit of $\tau_{\mathrm{KWW}}(q) \sim 10\,000$ ns on the range of relaxation times that we can report as numerical values. Spectra that have not decayed by at least 7% in our time window may give indications of still having a relax-

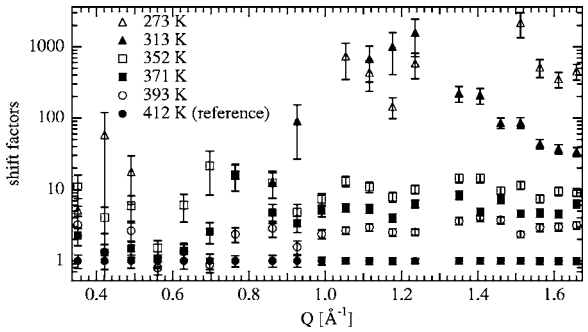

FIG. 4. Shift factors for the 30% blend. The reference temperature is T_0=412 K.

ation, but the relaxation time cannot be reasonably estimated.

The superposition of the spectra, obtaining a more complete decay curve, is performed by defining a shift factor

$$a_T = \frac{\tau(T)}{\tau(T_0)}. \tag{4}$$

Here $\tau(T)$ and $\tau(T_0)$ are the relaxation times at temperature T and a reference temperature T_0. In contrast to the treatment of pure polymers [35], we are not able to use shift factors from mechanical measurements because mechanical data do not superpose for this blend. Terminal relaxation times are available for each of the blend components, however because of the nature of the NSE experiment on perdeuterated blends we are not yet sure which component is being observed.

Figure 4 shows the shift factors for the 30% blend. The reference temperature is 412 K with fastest decay times. Where we have the most reliable data ($q>0.8$ Å^{-1}) the shift factors do not show significant q dependence. Error bars stand for one sigma statistical error. For the two lowest temperatures and for $q<0.8$ Å^{-1} there is more scatter on the data and the errors are certainly underestimated. This is essentially due to the small decay of the relaxation times thus being on the borderline of the instrument resolution, where instrumental systematic errors start to become very important. In the following we will use only points from $q>0.8$ Å^{-1}. Figure 5 shows the average of the shift factors weighted by the errors bars.

If we suppose an Arrhenius type temperature dependence of the relaxation times with activation energy E_A

$$\tau = \tau_0 \exp\left(\frac{E_A}{kT}\right). \tag{5}$$

Then the the shift factors in turn will become

$$a_T = \exp\left(-\frac{E_A}{kT_0}\right)\exp\left(\frac{E_A}{kT}\right). \tag{6}$$

As shown in Fig. 5 the temperature dependence of the shift factors is close to an activation energy description, though there seems to be a small systematic deviation. Such an Arrhenius behavior is suggestive of a β process, particularly when one considers that the lowest temperature shift factors are far *below* the blend T_g. Instead of taking the ratios of the relaxation times as done in Fig. 4, we can directly fit Eq. (5)

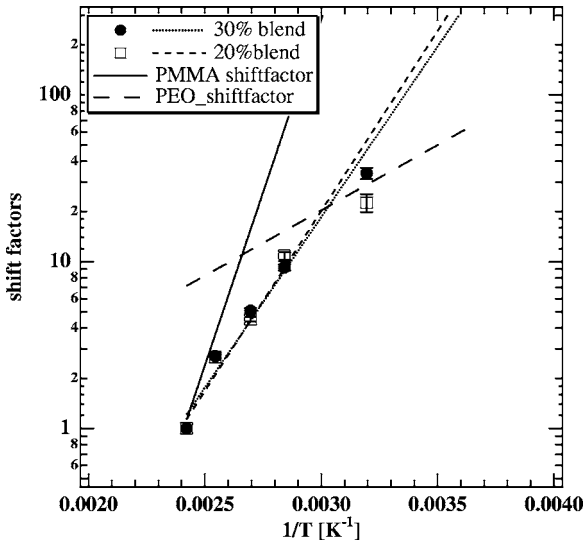

FIG. 5. Average shift factors for the blends. For the 10% blend only the three highest temperatures had measurable decay thus not giving sufficient range in $1/T$ for a meaningful fit. Dashed lines show activation energy fits. Solid line for comparison of the slope of the PMMA (79.4 kJ/mol) activation energy and long dashed line for PEO (15 kJ/mol) from Ref. [47].

for each q and take the average. This method yields similar activation energies with better statistics. Furthermore we obtain $\tau_0(q)$ which allow us to estimate the relaxation time for any temperature and q within the validity of Eq. (5). The activation energies are 43±1, 47±1 kJ/mol for the 30, 20 % blends, respectively. Within experimental accuracy the activation energy for the two blends can be considered to be the same. Its value is between the 79 kJ/mol, which is the activation energy of the local β process for pure PMMA [28] and 15 kJ/mol which is for PEO [47] as measured by dielectric relaxation. The above-mentioned systematic deviations could be viewed as a beginning of a cross over from the PMMA activation energy at high temperature toward the PEO activation energy at lower temperature. Such a shift with temperature would be expected if the PMMA segments become immobile within the time range of NSE at low T. As the shift factors were determined from the high q region, that is after the first correlation peak of the PMMA, it is not surprising that here the β relaxation might dominate. Furthermore from Fig. 1 we know that the relative contribution of PEO is the highest for $q>1.0$ Å^{-1} (up to 20% between q=1.2 and 1.66 Å^{-1}), thus a change in the apparent activation energy is not surprising. Here we have to mention the strong influence of the choice of the β exponent. Indeed the calculated activation energy for the two (30 and 20 %) blends become 32±1, 36±1 kJ/mol for β=0.4 and 66±1, 71±1 kJ/mol for β=0.2.

To check tTS, Eq. (4) can be used to shift the time scales and the spectra has to be divided by the fitted $A(q)$ prefactor of Eq. (3). Such scaled NSE spectra are shown in Fig. 6 for momentum transfer q=1.66 Å^{-1} for the three blends. Time-temperature superposition is reasonable at all momentum transfers, even when extended to $q<0.8$ Å^{-1}, although there due to the small decay of the curves the test is not very

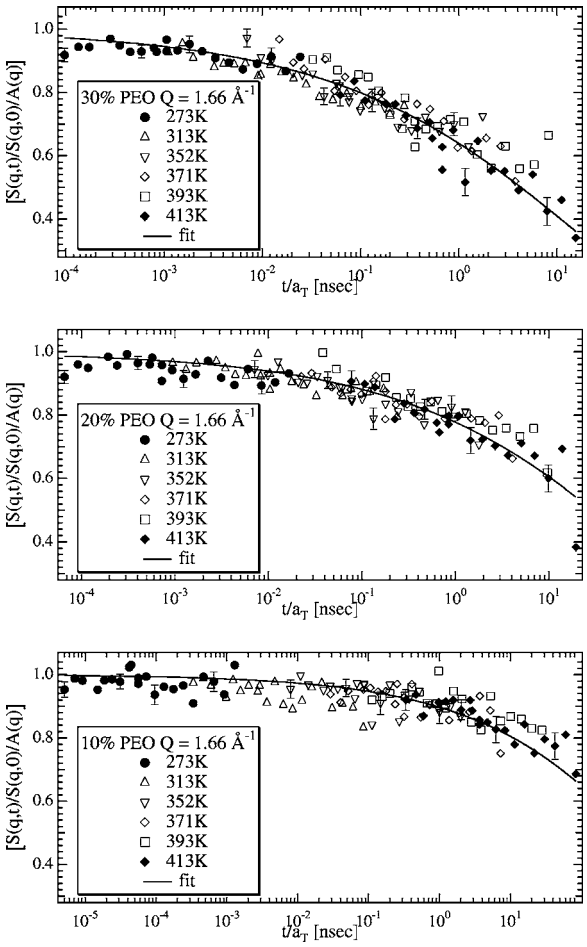

FIG. 6. Rescaled data with the calculated shift factor a_T of Eq. (4) for the 30% (a), 20% (b), and 10% (c) blend at $Q=1.66$ Å^{-1} and $T_0=352$ K. For clarity only some error bars (one sigma) are shown. Solid lines are the KWW fits Eq. (3) with $A(q)=1$.

stringent. It is important to keep in mind that the current experiments probe only a little more than two decades in time, whereas oscillatory shear measurements probe five, and thus present a far more rigorous test of time-temperature superposition. Also the two time windows are separated by seven decades and NSE probes at local spatial scales. It is conceivable that tTS holds for short time and small displacement, even though tTS clearly fails on long time and length scale.

C. Comparison of results with pure component data

Of interest when considering miscible blend dynamics is the difference of each component from its pure state. Although incoherent neutron scattering techniques can reveal the motion of each component by selective deuterium labeling, in the present system, coherent scattering is measured on perdeuterated polymers. As demonstrated by Eq. (2), a mixture of relaxation times is expected if the different components have different characteristic relaxation times. An additional complicating factor is that even single component polymers have strongly q-dependent collective relaxation times [37]. To orient ourselves, we compare relaxation times

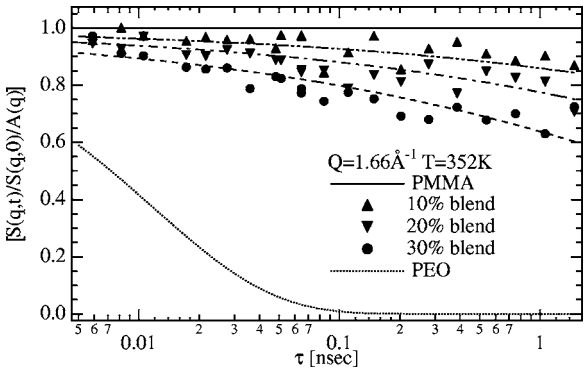

FIG. 7. Calculated spectra for the pure components and fitted curves for the blends at 1.66 Å^{-1} at $T=352$ K together with the measured data. These latters are divided by the fitted $A(q)$ prefactor of Eq. (3). Dashed and dashed-dotted lines are the fitted KWW functions as in Fig. 2 but with a prefactor $A(q)=1$.

obtained from our NSE measurements to those obtained from each pure component. We have measured the pure PMMA up to 413 K and at all q values the spectra were elastic in our time window with the exception of the two or three highest q values and highest temperatures. For the rest only the prefactor $A(q)$ of Eq. (3) shows q and temperature dependence but, as mentioned above, this reflects higher energy, probably local modes. For PEO, data are available at $T_g+127=348$ K [31,32]. From the published experimental values ($\tau=0.012$ ns and streching exponent $\beta=0.73$) we calculate the expected NSE curve in our time window and compare it to our blend results at the closest temperature of 352 K. This is shown in Fig. 7 as the dotted line, for the highest q value (1.66 Å^{-1}). The pure PMMA is completely elastic in this time window as shown by the $S(q,t)=1$ solid line. We now consider if we can observe any fraction of the PEO that behaves as the pure component. Even without fitting, it is clear that the blend curves cannot be decomposed into a sum of the pure components because the PMMA is too slow and the PEO is too fast. Furthermore, none of the experimental data (see, e.g., Fig. 6) show a partial fast decay. We have to note also that the pure PEO is not fast enough to be outside of our time window and contribute only to the prefactor $[A(q)<1]$ term of Eq. (3). This leads us to the conclusion that within experimental accuracy, and in the probed q (space) range, *we cannot detect any fraction of the pure PEO which would maintain the same mobility as the pure component neither do we see two well-separated relaxations which would correspond to the two components*. On the other hand, since none of the blend data decay completely within the time window, we cannot exclude the possibility that a small faction of the PMMA contributes some elastic scattering. Nevertheless in Fig. 6 at $q=1.66$ Å^{-1} where the decays are the most complete, there is no indication of such a tendency.

Another approach can be to consider the results at constant $T-T_g$. In Fig. 8 we compare our results to literature data on dielectric relaxation for the pure components [28,47] NSE results for coherent scattering of PEO [32] and incoherent QENS results on pure PMMA and the 20% blend [34]. We have chosen to show the values at $q=1.66$ Å^{-1} for several reasons. First we have the most confidence in our data at

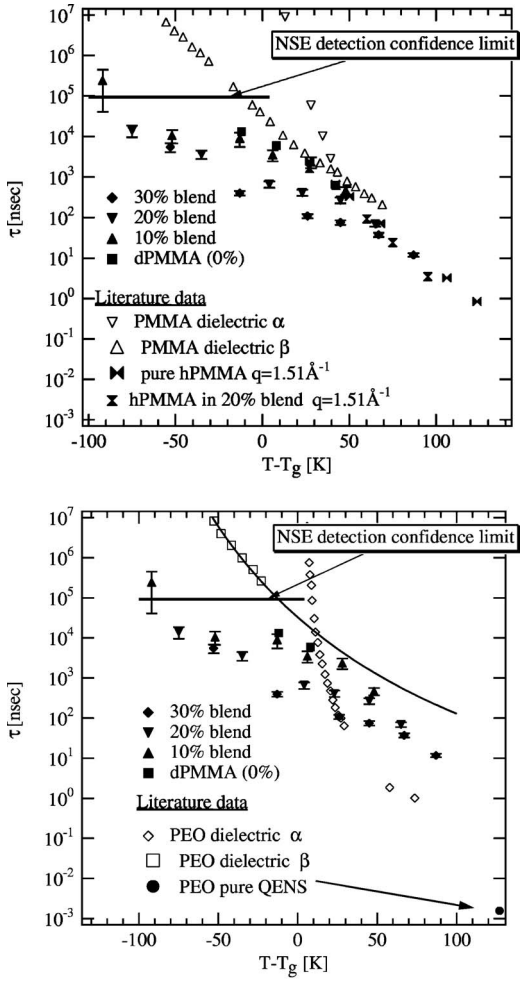

FIG. 8. Comparison of relaxation times of the blends from NSE (at $q=1.66$ Å^{-1}) with PMMA and PEOdynamics. QENS data for PEO are from Ref. [32], dielectric data for PEO from Ref. [47], for PMMA α and β relaxations from Ref. [28], and PMMA self-correlation (incoherent scattering) for pure PMMA and PEO-PMMA from Ref. [34]. Only some error bars are shown.

high q because the relaxations are the most pronounced. Here the relaxation times for coherent, incoherent neutron scattering, and dielectric relaxations are very close to each other on an absolute scale, thus comparison is easier. Even the pure dPMMA at the two highest temperature $T-T_g=-12$ and 8 K gave exploitable results. Finally the static scattering data (Fig. 1) indicate that we have the most contribution from the PEO at the highest q values. One more caution has to be taken when comparing different data. As mentioned already the values of the fitted relaxation times are strongly correlated with the values of the β exponent in Eq. (3). To compensate for this effect we calculate the average relaxation times [Ref. [48], Eq (4.4)]

$$\langle \tau(q) \rangle = \frac{\Gamma\left(\frac{1}{\beta}\right)}{\beta} \tau_{\mathrm{KWW}}(q). \tag{7}$$

In Fig. 8 the thick horizontal line indicates the experimental upper confidence limit we set for the relaxation times, upscaled by Eq. (7). Plotting the average relaxation time as a function of $T-T_g$ brings them closer but there appears to remain a systematic change by composition. Increasing PEO content makes the relaxation faster than one would expect only from the change of T_g. This is in contrast with the finding of the self-relaxation of PMMA in the blend where scaling with the change in T_g was found [34]. It is possible that we are observing a mixing of relaxations times as shown in Eq. (2). We have to stress that we definitively do see deviation from elastic scattering below T_g even for the pure dPMMA sample, although close to resolution limit. The $q=1.66$ Å^{-1} value is already beyond the first correlation peak so it is not very surprising that the β relaxations start to dominate. Such phenomena has been observed already for polybutadiene [2]. The temperature dependence around T_g of the relaxation times is very similar to the dielectric β relaxations independently whether we compare to PEO or PMMA. We want to stress again, the fact that the absolute values of the relaxations times are close to each other is to some extent accidental. (See later in Fig. 9 the strong q dependence.) Here our aim was to compare the temperature dependences around T_g. If the β relaxation is becoming the dominant than it is not surprising that the relaxation times do not scale with $T-T_g$ as β is not expected to be influenced by blending.

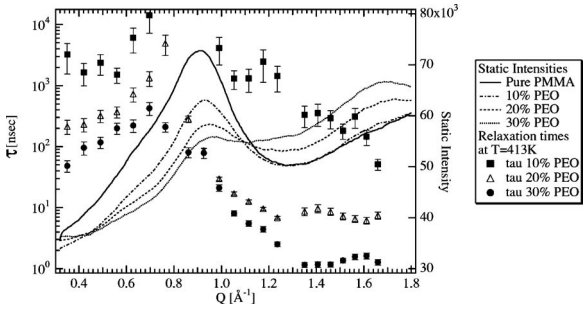

FIG. 9. Relaxation times at 413 K and static structure factors of the pure PMMA and the three blends. Missing points in the 0.8 Å$^{-1}<q<1$ Å^{-1} for the 10% blend gave relaxation times $>10\,000$ ns (not shown).

Figure 9 shows the relaxation time at the highest temperature as a function of q for the three blends, together with the static structure factors in the same q range. There is a modulation of τ roughly in phase with the static intensity. However relaxation times vary by more than two orders of magnitude between 0.8 and 1.4 Å^{-1} and also by more than a factor 10 between 0.4 and 0.8 Å^{-1}, both are thus probably too much to be accounted for by the well-known deGennes narrowing [49] as the modulation in $S(q)$ is at most a factor two. Its applicability to amorph polymers to the best of our knowledge is not a solved problem. Using the ansatz of Skold [50], qualitative agreement was found in the case of a homopolymer [37]. The extension to blends would need at least the knowledge of the incoherent relaxation times and most likely some theoretical framework.

For completeness in Fig. 10 we show the q, temperature, and composition dependence of the prefactor $A(q)$ of Eq. (3). As has been found in many glassy systems it is also modulated in phase with the static structure factor. The element in this figure is that with increasing PEO content it becomes

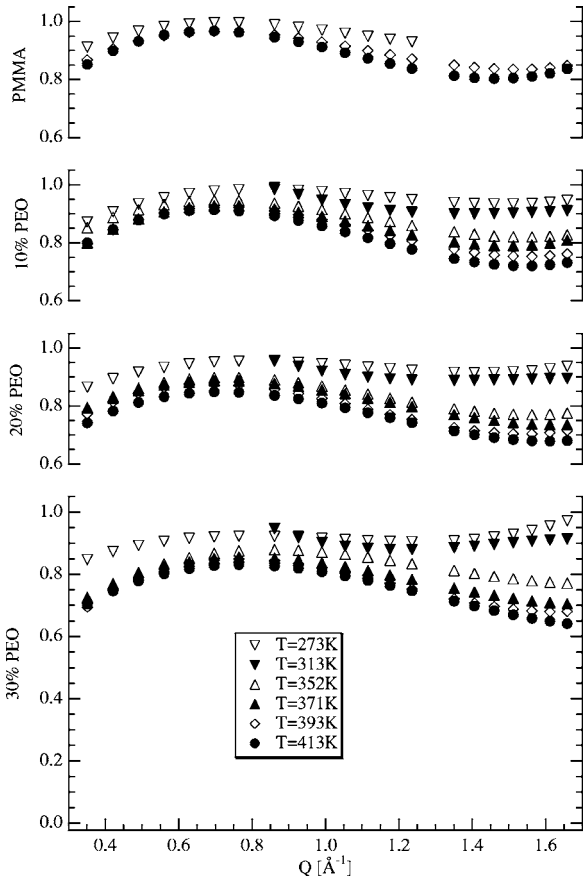

FIG. 10. q and temperature dependence of the prefactor $A(q)$ of Eq. (3), for the pure PMMA, 10, 20, and 30 % blends.

smaller. The effect of blending thus is not only changing the relaxation times but also increasing the density of states in the 0.2–2.5 meV (and possibly higher) energy range, which is usually attributed to local motions. Again at least two scenarios can be imagined. Either the presence of PEO facilitates the local motions even for PMMA which are usually attributed to this energy range, or this fast motion contribution comes from the PEO itself. Interestingly, at any given q and temperature, the amount of relaxation that is too fast for our time window $(1-A)$ roughly scales with the PEO content.

V. CONCLUSIONS

We have investigated the dynamics of 10, 20, and 30 % dPEO/dPMMA blends at six temperatures below and above the blend T_g and at wave vectors ranging from 0.35 to 1.66 Å^{-1} using the NSE technique, which provides both time and spatial resolution. Due to the large difference in the pure component glass transitions, we are able to conclusively show that no significant fraction of the fast component (PEO) has the same mobility at a given temperature as in its pure form and we saw no evidence for two well-separated relaxation time which would correspond to the two components. Because of the limited time window we cannot make such a strong statement for the mobility of the PMMA. As it is the dominant component, to account for the observed relaxations at least some of the PMMA is more mobile than the pure component at the same temperature. Furthermore the change in the glass transition temperature with blending is not sufficient to account for the change in relaxation times as shown in Fig. 8.

The decay curve of the relaxations is rather stretched with an exponent $\beta \sim 0.30$ and the temperature dependence is compatible with an Arrhenius activation energy of around 42–45 kJ/mol. This information we could verify with good accuracy only for $q > 1.0$ Å^{-1}. Since the observed relaxation persists also far below the blend T_g, it is likely dominated by the β relaxation of PMMA. The relaxation times are strongly q dependent, mimicking the static structure factor, but the q dependence is too strong to be explained by deGennes narrowing.

Further measurements with even higher resolution would be desirable, in particular on samples with one or the other component labeled by hydrogen. Unfortunately present instrument performances make it unlikely to be able to perform such experiments in the near future.

ACKNOWLEDGMENTS

Financial support for this work [J.K.M.] was provided by the National Science Foundation, Polymers Program, through a CAREER Grant No DMR-0134910. DMR-9977928 and INT-9800092 allowed R.H.C. and S.K. to travel to Grenoble for the NSE measurements. We would like to thank T. Hansen at the ILL who give us some beam time on D20 to measure the static structure factors.

[1] D. Gomez, A. Alegria, K. Arbe, and J. Colmenero, Macromolecules **34**, 503 (2001).
[2] A. Arbe, D. Richter, J. Colmenero, and B. Farago, Phys. Rev. E **54**, 3853 (1996).
[3] T. W. N. Bieze, J. R. C. Vandermaarel, C. D. Eisenbach, and J. C. Leyte, Macromolecules **27**, 1355 (1994).
[4] W. Zhu, D. J. Gisser, and M. D. Ediger, J. Polym. Sci., Part B: Polym. Phys. **32**, 2251 (1994).
[5] A. S. Merenga, C. M. Papadakis, F. Kremer, J. Liu, and A. F. Yee, Colloid Polym. Sci. **279**, 1064 (2001).
[6] A. Arbe, M. Monkenbusch, J. Stellbrink, D. Richter, B. Farago, K. Almdal, and R. Faust, Macromolecules **34**, 1281 (2001).
[7] T. Kanaya and K. Kaji, in *Polymer Physics and Engineering*, Vol. 154 of Advances in Polymer Science (Springer-Verlag, Berlin, 2001), pp. 87–141.
[8] B. Ewen and D. Richter, in *Neutron Spin Echo Spectroscopy Viscoelasticity Rheology, Vol. 134 of Advances in Polymer Science* (Springer-Verlag, Berlin, 1997) pp. 1–129.
[9] R. H. Colby, Polymer **30**, 1275 (1989).

[10] D. Richter, M. Monkenbusch, A. Arbe, J. Colmenero, and B. Farago, Physica B **241**, 1005 (1997).
[11] A. Alegria, J. Colmenero, K. L. Ngai, and C. M. Roland, Macromolecules **27**, 4486 (1994).
[12] S. K. Kumar, R. H. Colby, S. H. Anastasiadis, and G. Fytas, J. Chem. Phys. **105**, 3777 (1996).
[13] I. Cendoya, A. Alegria, J. M. Alberdi, J. Colmenero, H. Grimm, D. Richter, and B. Frick, Macromolecules **32**, 4065 (1999).
[14] A. Arbe, A. Alegria, J. Colmenero, S. Hoffmann, L. Willner, and D. Richter, Macromolecules **32**, 7572 (1999).
[15] S. Hoffmann, L. Willner, D. Richter, A. Arbe, J. Colmenero, and B. Farago, Phys. Rev. Lett. **85**, 772 (2000).
[16] M. Doxastakis, M. Kitsiou, G. Fytas, D. N. Theodorou, N. Hadjichristidis, G. Meier, and B. Frick, J. Chem. Phys. **112**, 8687 (2000).
[17] R. E. Wetton, W. J. Macknight, J. R. Fried, and F. E. Karasz, Macromolecules **11**, 158 (1978).
[18] P. S. Alexandrovich, F. E. Karasz, and W. J. Macknight, J. Macromol. Sci., Phys. **B17**, 501 (1980).
[19] C. M. Roland and K. L. Ngai, Macromolecules **25**, 363 (1992).
[20] G. Katana, F. Kremer, E. W. Fischer, and R. Plaetschke, Macromolecules **26**, 3075 (1993).
[21] A. Zetsche and E. W. Fischer, Acta Polym. **45**, 168 (1994).
[22] R. Mukhopadhyay, A. Alegria, J. Colmenero, and B. Frick, J. Non-Cryst. Solids **235**, 233 (1998).
[23] C. M. Roland and K. L. Ngai, Macromolecules **24**, 2261 (1991).
[24] J. A. Zawada, C. M. Ylitalo, G. G. Fuller, R. H. Colby, and T. E. Long, Macromolecules **25**, 2896 (1992).
[25] G. Katana, E. W. Fischer, T. Hack, V. Abetz, and F. Kremer, Macromolecules **28**, 2714 (1995).
[26] T. Lodge and T. Mcleish, Macromolecules **33**, 5278 (2000).
[27] H. Ito, T. P. Russell, and G. D. Wignall, Macromolecules **20**, 2213 (1987).
[28] R. Bergman, F. Alvarez, A. Alegria, and J. Colmenero, J. Chem. Phys. **109**, 7546 (1998).
[29] T. R. Lutz, Y. Y. He, M. D. Ediger, H. H. Cao, G. X. Lin, and A. A. Jones, Macromolecules **36**, 1724 (2003).
[30] M. Dionisio, A. C. Fernandes, J. F. Mano, N. T. Correia, and R. C. Sousa, Macromolecules **33**, 1002 (2000).
[31] G. M. Mao, R. F. Perea, W. S. Howells, D. L. Price, and M. L. Saboungi, Nature (London) **405**, 163 (2000).
[32] G. M. Mao, M. L. Saboungi, D. L. Price, M. Armand, F. Mezei, and S. Pouget, Macromolecules **35**, 415 (2002).
[33] B. Mos, P. Verkerk, S. Pouget, A. van Zon, G. J. Bel, S. W. de Leeuw, and C. D. Eisenbach, J. Chem. Phys. **113**, 4 (2000).
[34] V. Sakai, C. Chen, and J. K. Maranas, Macromolecules **37**, 9975 (2004).
[35] D. Richter, A. Arbe, J. Colmenero, M. Monkenbusch, B. Farago, and R. Faust, Macromolecules **31**, 1133 (1998).
[36] A. Arbe, D. Richter, J. Colmenero, and B. Farago, Physica B **234**, 437 (1997).
[37] B. Farago, A. Arbe, J. Colmenero, R. Faust, U. Buchenau, and D. Richter, Phys. Rev. E **65**, 051803 (2002).
[38] V. Arrighi, C. Pappas, A. Triolo, and S. Pouget, Physica B **301**, 157 (2001).
[39] F. Mezei, in *Neutron Spin Echo*, Lecture Notes in Physics Vol. 28, edited by F. Mezei, pp. 3–26.
[40] B. Farago, Physica B **241**, 113 (1997).
[41] B. Farago, ILL Annual Report (Institute Laue Langevin, Grenoble, 1988), pp. 103–106.
[42] B. Farago, in *Neutron Spin Echo Spectroscopy*. Basics, Trends and Applications, Lecture Notes in Physics Vol. 601, edited by F. Mezei, C. Pappas, and T. Gutberlet (Springer Verlag, Berlin, 2003).
[43] A. J. Moreno, A. Alegria, J. Colmenero, and B. Frick, Macromolecules **34**, 4886 (2001).
[44] K. Schmidt-Rohr, A. S. Kulik, H. W. Beckham, A. Ohlemacher, U. Pawelzik, C. Boeffel, and H. W. Spiess, Macromolecules **27**, 4733 (1994).
[45] J. A. Johnson, M. L. Saboungi, D. L. Price, S. Ansell, T. P. Russell, J. W. Halley, and B. Nielsen, J. Chem. Phys. **109**, 7005 (1998).
[46] S. W. de Leeuw, A. Van Zon, and G. J. Bel, Electrochim. Acta **46**, 1419 (2001).
[47] X. Jin, S. H. Zhang, and J. Runt, Polymer **43**, 6247 (2002).
[48] D. Richter, M. Monkenbusch, J. Allgeier, A. Arbe, J. Colmenero, B. Farago, Y. C. Bae, and R. Faust, J. Chem. Phys. **111**, 6107 (1999).
[49] P. G. Degennes, Physica (Amsterdam) **25**, 825 (1959).
[50] K. Skold, Phys. Rev. Lett. **19**, 1023 (1967).